THE JOURNAL OF BIOLOGICAL CHEMISTRY VOL. 290, NO. 9, pp. 5772–5782, February 27, 2015

A Unique Phenylalanine in the Transmembrane Domain Strengthens Homodimerization of the Syndecan-2 Transmembrane Domain and Functionally Regulates Syndecan-2*

Received for publication, July 25, 2014, and in revised form, January 8, 2015 Published, JBC Papers in Press, January 8, 2015, DOI 10.1074/jbc.M114.599845

Mi-Jung Kwon[‡], Youngsil Choi[‡], Ji-Hye Yun[§1], Weontae Lee[§], Inn-Oc Han[¶], and Eok-Soo Oh[‡2]

From the [‡]Department of Life Sciences, Research Center for Cellular Homeostasis, Ewha Womans University, Seoul 120-750, Korea, the [§]Department of Biochemistry, College of Life Science and Biotechnology, Yonsei University, Seoul 120-749, Korea, and the [¶]College of Medicine, Department of Physiology and Biophysics, Inha University, Incheon 402-751 Korea

Background: The transmembrane domains of syndecan family members harbor a G*XXX*G motif forming non-covalently linked SDS-resistant dimers.
Results: A unique phenylalanine in the syndecan-2 transmembrane domain contributes to its transmembrane homointeraction and unique functions.
Conclusion: A unique phenylalanine in syndecan-2 endows its transmembrane domain with specific functions.
Significance: This report provides insight into the importance of the transmembrane domain for syndecan receptor function.

The syndecans are a type of cell surface adhesion receptor that initiates intracellular signaling events through receptor clustering mediated by their highly conserved transmembrane domains (TMDs). However, the exact function of the syndecan TMD is not yet fully understood. Here, we investigated the specific regulatory role of the syndecan-2 TMD. We found that syndecan-2 mutants in which the TMD had been replaced with that of syndecan-4 were defective in syndecan-2-mediated functions, suggesting that the TMD of syndecan-2 plays one or more specific roles. Interestingly, syndecan-2 has a stronger tendency to form sodium dodecyl sulfate (SDS)-resistant homodimers than syndecan-4. Our structural studies showed that a unique phenylalanine residue (Phe^{167}) enables an additional molecular interaction between the TMDs of the syndecan-2 homodimer. The presence of Phe^{167} was correlated with a higher tendency toward oligomerization, and its replacement with isoleucine significantly reduced the SDS-resistant dimer formation and cellular functions of syndecan-2 (*e.g.* cell migration). Conversely, replacement of isoleucine with phenylalanine at this position in the syndecan-4 TMD rescued the defects observed in a mutant syndecan-2 harboring the syndecan-4 TMD. Taken together, these data suggest that Phe^{167} in the TMD of syndecan-2 endows the protein with specific functions. Our work offers new insights into the signaling mediated by the TMD of syndecan family members.

Transmembrane domain (TMD)[3]-mediated association is the important process through which integral membrane receptors can stimulate a series of signaling events inside the cell. For most membrane receptors, TMD-mediated association is initiated by the binding of a ligand to the extracellular domain of the receptor. This induces the TMD helices to approach one another and facilitates the clustering of the cytoplasmic domains, thereby activating intracellular signaling (1, 2). Although the fundamental importance of the TMD is well recognized, we do not yet have a clear molecular understanding of the mechanisms underlying TMD-TMD interactions or how TMD-mediated signal transduction regulates cellular functions.

Recent investigations have explored the regulatory mechanisms of membrane receptors by studying TMD-TMD interactions (3). One of the best-studied examples is glycophorin A (GpA). The GpA TMD induces non-covalent dimerization through a G*XXX*G motif of its right-handed transmembrane helix. The two GpA TMDs come close enough to allow the formation of van der Waals interactions between their G*XXX*G motifs, stabilizing the dimer with sufficient affinity that it resists dissociation in the presence of detergents, such as during SDS-PAGE. This is called SDS-resistant dimer formation (4, 5).

The TMD of the M13 bacteriophage (MCP-TMD) also has a helical G*XXX*G motif, but it forms a homointeraction that is weaker than that of GpA (6). Melnyk *et al.* (7) reported that this is because interfacial residues around G*XXX*G motif also contribute to TMD-TMD affinity. Similarly, other researchers have reported that residues around the G*XXX*G motif participate in TMD-mediated aromatic and cation-π interactions, helping to

* This work was supported by National Research Foundation of Korea (NRF) Grants 2012R1A5A1048236 and 2013R1A2A2A01013565 (to E. S. O.) funded by the Korean government (MSIP) and Mid-career Researcher Program Grant NRF-2013R1A2A2A01068963 through an NRF grant funded by the Korean Ministry of Education, Science, and Technology (MEST) (to W. T. L.).
[1] Recipient of a Brain Korea Plus (BK+) grant.
[2] To whom correspondence should be addressed: Dept. of Life Sciences, Ewha Womans University, 52, Ewhayeodae-gil, Seodaemoon-Gu, Seoul 120-750 Korea. Tel.: 82-2-3277-3761; Fax: 82-2-3277-3760; E-mail: OhES@ewha.ac.kr.

[3] The abbreviations used are: TMD, transmembrane domain; PBD, PAK1 binding domain; PDGFR, platelet-derived growth factor receptor; SDC, syndecan; GpA, glycophorin A; REF, rat embryonic fibroblast; NTA, nitrilotriacetic acid; 2TM, TMD of syndecan-2; 2eTC, transmembrane and cytosolic domains of syndecan-2; CFP, cyan fluorescent protein.

stabilize the TMD homodimer (8). Therefore, this TMD-TMD association appears to be regulated by the G*XXX*G motif and its surrounding amino acid residues, and this might affect TMD-mediated signal transduction.

The syndecans are a family of transmembrane heparan sulfate proteoglycans that regulate diverse cellular functions (9). The four family members (syndecan-1, -2, -3, and -4) are single transmembrane domain receptors that comprise an extracellular domain, a cytoplasmic domain, and a TMD (9). The extracellular domains of the syndecan family members interact with numerous matrix molecules and growth factors (10, 11). For example, interactions with core protein or glycosaminoglycan, which attach to the extracellular domain, activate syndecans to regulate cell signals, leading to cytoskeletal reorganization, cell adhesion, and cell migration (9, 11, 12).

All syndecans contain G*XXX*G motifs and form SDS-resistant homodimers (13, 14). The TMD is sufficient for syndecan dimerization, and experiments using a syndecan mutant in which the glycines of the G*XXX*G motif were mutated to leucines showed that syndecan dimerization is mediated by this motif (13). Furthermore, the syndecan TMD-TMD interaction was found to critically regulate the various functions of the syndecan family members (13). For example, whereas wild-type syndecan-4 can regulate cytoskeletal organization, its dimerization-deficient mutant showed decreased binding with α-actinin and less activation of PKCα and RhoA (15, 16). The TMD-TMD association is also important for syndecan-2-mediated functions, including the activation of Rac in colon cancer, increased cell migration, and the interaction with syntenin (17, 18).

Interestingly, a previous study using synthetic peptides showed that the syndecan TMDs have different dimerization affinities (14). This suggests that other residues of the syndecan TMD, beyond the G*XXX*G motif, might participate in the TMD-TMD association and related syndecan functions. Here, we show for the first time that the TMD of syndecan-2 has a higher affinity for homodimerization than the syndecan-4 TMD and that this difference in TMD affinity endows syndecan-2 with its specific functions.

EXPERIMENTAL PROCEDURES

Antibodies and Materials—Monoclonal anti-GST, -ERK, and -phospho-ERK, and polyclonal anti-His were purchased from Santa Cruz Biotechnology, Inc. Polyclonal anti-Rac1 was purchased from Millipore (Billerica, MA). Fibronectin was obtained from Upstate Biotechnology, Inc. (Lake Placid, NY). Transient transfections were carried out using Vivamagic (Vivagen, Seongnam, Korea), as described in the provided protocol. Monoclonal (mAb) antibody to syndecan-2 (SDC2) was produced by AdipoGen (Incheon, Korea) (19).

Cell Culture—Rat embryonic fibroblasts (REFs) were maintained in α-modified Eagle's medium (Invitrogen) supplemented with 5% (v/v) fetal bovine serum (FBS) (GE Healthcare), and gentamycin (50 μg/ml) (Sigma-Aldrich). HCT116 cells were maintained in McCoy's 5a medium (Welgene, Daegu, Korea). HEK293T cells were maintained in Dulbecco's modified Eagle's medium (DMEM; Invitrogen) supplemented with 10% (v/v) FBS and gentamycin (50 μg/ml). All cell lines were maintained at 37 °C in a humidified 5% CO_2 atmosphere.

Construction and Transfection of Expression Vectors—The extracellular and transmembrane domains (amino acids 151–179 and 146–174) of rat syndecan-2 or rat syndecan-4 were linked with the cytoplasmic domain of human PDGFR (amino acids 557–1107) to generate chimeric proteins, 2eTPC and 4eTPC, respectively. The extracellular and cytoplasmic domains of syndecan-2 (amino acids 1–154 and 180–211) were linked with the TMD of syndecan-4 (amino acids 150–174) to create a chimeric protein designated 2E4T2C, whereas the extracellular and cytoplasmic domains of syndecan-4 (amino acids 1–149 and 175–202) were linked with the TMD of syndecan-2 (amino acids 155–179) to generate chimeric protein 4E2T4C (13). Single point mutants in the TMDs of syndecan-2 or -4 (*i.e.* S2(F167Y), S2(F167I), S2(F169Y), S2(F172Y), 2E4T2C(I162F), and S4(I162F)) (Fig. 3*A*) were constructed by commercial gene synthesis (Bioneer, Daejeon, Korea). The chimeras or point mutants were inserted into the N-terminal HA-tagging pcDNA3 expression vector (Invitrogen). HEK293T cells (6.0×10^5 cells/well), REFs (8.0×10^4 cells/well), and HCT116 cells (1.0×10^6 cells/well) were plated on 6-well plates, incubated at 37 °C for 24 h, and then transfected with the generated expression vectors, as described in the Vivagen protocol.

RNA Extraction and Reverse Transcription Polymerase Chain Reaction (RT-PCR)—Total RNA, which was extracted with TRIzol reagent (Invitrogen) following the manufacturer's protocols, was used as template for a reverse transcriptase reaction. Aliquots of cDNA were amplified using the following primers: rat SDC2, 5′-ATGCGGGTACGAGCCACGTC-3′ (forward) and 5′-CGGGAGCAGCACTAGTGAGG-3′ (reverse); human SDC2, 5′-ACATCTCCCCTTTGCTAACGGC-3′ (forward) and 5′-TAACTCCATCTCCTTCCCCAGG-3 (reverse); human GAPDH, 5′-CCACCCATGGCAAATTCCATGGCA-3′ (forward) and 5′-TCTAGACGGCAGGTCAGGTCCACC-3′ (reverse); human/rat β-actin, 5′-TGGAATCCTGTGGCATCCATGAAA-3′ (forward) and 5′-TAAAACGCAGCTCAGTAACAGTCCG-3′ (reverse); rat integrin α5, 5′-CCCTCGTTTACACATGCCCT-3′ (forward) and 5′-ATGAATCTTTGCAGGCGGGA-3′ (reverse); rat/human integrin α2, 5′-GGC ATT GAA AAC ACT CGA T-3′ (forward) and 5′-TCG GAT CCC AAG ATT TTC TG-3′ (reverse); integrin β1, 5′-ACA AGA GTG CCG TGA CAA CT-3′ (forward) and 5′-AGC TTG ATT CCA AGG GTC CG-3′ (reverse). After an initial denaturation for 5 min at 94 °C, an amplification profile including 30 cycles of denaturation for 30 s at 94 °C, annealing for 60 s at 58 °C (for rat SDC2, human GAPDH, and human/rat β-actin), 55 °C (for human SDC2), or 54 °C (for integrins), and extension for 60 s at 72 °C was performed. The reaction products were analyzed in 1% agarose gels.

Immunoblotting—Cultures were washed twice with PBS, and the cells were lysed in radioimmune precipitation assay buffer (50 mM Tris, pH 8.0, 150 mM NaCl, 1% Nonidet P-40, 10 μM NaF, and 2 μM Na_3VO_4) containing a protease inhibitor mixture (1 μg/ml aprotinin, 1 μg/ml antipain, 5 μg/ml leupeptin, 1 μg/ml pepstatin A, and 20 μg/ml phenylmethylsulfonyl fluoride). Cell lysates were clarified by centrifugation at 13,000 rpm for 15 m at 4 °C, denatured with SDS-PAGE sample buffer,

boiled, and analyzed by SDS-PAGE. Proteins were transferred to polyvinylidene difluoride (PVDF) membranes (Amersham Biosciences) and probed with the appropriate antibodies. Signals were detected by enhanced chemiluminescence (ECL; Abclon, Seoul, Korea).

Expression and Purification of Recombinant GST-Syndecan Core Proteins—The cDNAs encoding full-length rat SDC2 and SDC4, the substituted TMD mutants (2E4T2C, 4E2T4C, 2EPT2C, and 4EPT4C), or the single point mutants (S2(F167Y), S2(F167I), S2(F169Y), S2(F172Y), 2E4T2C(I162F), and S4(I162F)) were synthesized by PCR and subcloned into the GST expression vector, pGEX-5X-1 (Amersham Biosciences). These constructs were used to transform *Escherichia coli* DH5α, and the expression of GST fusion proteins was induced by incubation with 1 mM isopropyl-β-D-thiogalactopyranoside for 4 h at 37 °C. The fusion proteins were purified with glutathione-agarose beads (GE Healthcare), as described previously (13).

Expression and Purification of Recombinant His-Syndecan Core Proteins—The cDNAs encoding the full-length rat syndecan-2 or -4 core proteins, the substituted TMD mutants (2E4T2C and 4E2T4C), or the single point mutants (S2(F167Y), S2(F167I), S2(F169Y), S2(F172Y), 2E4T2C(I162F), and S4(I162F)) were synthesized by PCR and subcloned into the His-tagging expression vector, pET32a$^+$ (Novagen, Madison, WI). The expression of fusion proteins in *E. coli* BL21 was induced by incubation with 0.3 mM isopropyl-β-D-thiogalactopyranoside at 30 °C for 16 h. The *E. coli* cells were lysed with lysis buffer (20 mM Na_2HPO_4, pH 8.0, 150 mM NaCl, 5 mM β-mercaptoethanol, and 0.5% Triton X-100) containing a protease inhibitor mixture, with sonication on ice for 1 min. The insoluble material was removed by centrifugation at 13,000 $\times$ *g* for 30 min at 4 °C, and the supernatants containing His-syndecan fusion proteins were applied to Ni^{2+}-NTA-agarose columns (Qiagen, Hilden, Germany). Each column was washed three times with lysis buffer containing 50 mM imidazole, and the bound proteins were eluted with lysis buffer containing 500 mM imidazole.

NMR Sample Preparation and NMR Titration—The TMD of rat syndecan-2 (2TM) was subcloned into the pET32a$^+$ vector (Novagen), which encodes a His-Trx fusion tag with an enterokinase enzyme recognition site in front of the target protein, allowing the His-Trx tag to be removed during protein purification. The transmembrane and cytosolic domains of syndecan-2 (2eTC) and its single point mutant, F167I, were subcloned in the same manner. Fusion proteins were highly expressed in *E. coli* BL21 (DE3) cells (Novagen) via induction with 1 mM isopropyl-β-D-thiogalactopyranoside at 25 °C for 18 h and then harvested. For protein purification, each frozen cell pellet was lysed with lysis buffer (50 mM Tris-HCl, pH 8.0, 150 mM NaCl, and 5 mM β-mercaptoethanol) and subjected to sonication. The sample was centrifuged at 13,000 $\times$ *g* for 30 min. The insoluble fraction (pellet) was resolubilized using refolding buffer (50 mM Tris-HCl, pH 8.0, 150 mM NaCl, 5 mM β-mercaptoethanol, and 1% *n*-dodecyl β-D-maltoside) (Affymetrix, Santa Clara, CA) and loaded onto an Ni^{2+}-NTA affinity column (GE Healthcare). The column was washed twice (50 mM Tris-HCl, pH 8.0, 150 mM NaCl, 5 mM β-mercaptoethanol, 20 mM imidazole, and 0.1% *n*-dodecyl β-D-maltoside), and the target protein was eluted (50 mM Tris-HCl, pH 8.0, 150 mM NaCl, 5 mM β-mercaptoethanol, 250 mM imidazole, and 0.05% *n*-dodecyl β-D-maltoside). The imidazole was removed with a PD-10 desalting column (GE Healthcare), and the fusion tag was removed by enterokinase treatment followed by purification with a reverse Ni-NTA affinity column. The target protein was dialyzed against 20 mM ammonium bicarbonate and finally lyophilized to a high concentration (5 mg/ml). For ^{13}C and ^{15}N isotope labeling of the target protein, [^{13}C]glucose and $^{15}NH_4Cl$ (Cambridge Isotope Inc., Andover, MA) were added to the M9 minimal medium during protein expression.

For NMR experiments, proteins were resuspended in 10 mM Na_2HPO_4, pH 7.0, 4 mM DTT, 1 mM sodium azide, 100 mM dodecylphosphocholine (DPC), and 90% H_2O, 10% D_2O. All NMR spectra were obtained at 318 K on a Bruker DRX 900-MHz spectrometer with a Cryoprobe (Division of Magnetic Resonance, Korea Basic Science Institute (KBSI), Ochang, Chungbuk, Korea) and processed and analyzed using the NMRPipe/NMRDraw (Biosym/Molecular Simulation, Inc. San Diego, CA) and Sparky programs (University of California, San Francisco, CA). Sequential backbone resonance assignment was executed by data from ^1H-^{15}N heteronuclear single quantum coherence, three-dimensional HNCACB, CBCACONH, and HNCO experiments. NMR titrations were performed using ^{15}N-labeled 2TM and unlabeled 2eTC or 2eTC (F167I) proteins at different molar ratios (1:1, 1:2, and 1:3). Chemical shift change values were calculated using the equation, $\Delta\delta_{AV} = ((\Delta\delta_{1H})^2 + (\Delta\delta_{15N}/5)^2)^{1/2}$, $\Delta\delta_{AV}$, $\Delta\delta_{1H}$, and $\Delta\delta_{15N}$ represent average chemical shift value, proton chemical shifts, and nitrogen chemical shift changes, respectively.

Analytical Size Exclusion Gel Chromatography—The structural conformations of both 2eTC and 2eTC(F167I) proteins were confirmed using the ACQUITY UPLC system (Waters, Milford, MA) and BEH 200 columns (Waters). The columns were equilibrated in 50 mM HEPES (pH 7.5), 150 mM NaCl, 0.05% *n*-dodecyl β-D-maltoside, 0.01% cholesterol hemisuccinate, and the proteins (1.4 mg/ml) were loaded into the column at a flow rate of 0.3 ml/m. The oligomeric states of proteins were detected and analyzed by absorption of ultraviolet light at a wavelength of 280 nm. The column was calibrated using BEH200 SEC protein standard mix (P/N 186006518).

Construct of Vector and Förster Resonance Energy Transfer (FRET)—Control DNA construct pECFP-YFP, a construct of SDC3-YFP and SDC3-CFP, was kindly provided by Prof. Heikki Rauvala (Neuroscience Center, University of Helsinki) (20). Rat SDC2 or SDC4 cDNA was ligated into the provided expression vector. HEK 293T cells were co-transfected with the indicated cDNAs, fixed for 10 min in 3.5% paraformaldehyde, washed with PBS, and imaged on a Zeiss Axiovert 200 M inverted microscope equipped with a Zeiss 510 Meta confocal (Carl Zeiss) head using plan-apochromat $\times$63, 1.4 numeric aperture oil with a differential interference contrast capability lens. A 458-nm argon laser light/Meta detector (420 nm) for CFP channel excitation and emission, a 514-nm argon laser light/Meta detector (530–600 nm) for YFP channel excitation and emission, and a 458-nm argon laser light/Meta detector (530–600 nm) for FRET channel excitation and emission were used.

Flow Cytometry—Transfected REF cells were harvested with 5 mM EDTA and 5% FBS in PBS, washed twice with PBS, aliquoted, and incubated separately with SDC2 antibodies. After incubating for 16 h at 4 °C, cells were washed three times with PBS containing 0.05% Tween 20 and stained with FITC-conjugated secondary antibodies (Abclone). After a 1-h incubation in the dark, cells were washed three times with PBS and resuspended in PBS. Fluorescence was then measured by flow cytometry using FACSCalibur (BD Biosciences) and analyzed with CellQuestPro software (BD Biosciences).

Inverted Centrifugal Detachment Assay—Cell-substratum adhesiveness was quantified using an inverted centrifugal detachment assay. Fibronectin was diluted in PBS (10 μg/ml), added to the 12-well plate, and incubated at 37 °C for 1 h. The plates were then washed with PBS and blocked with 0.2% heat-inactivated BSA at room temperature for 1 h. Transfected cells (8.0×10^4 cells/well) in serum-free medium were then added to a coated plate and incubated for an additional 2 h at 37 °C in 5% CO_2. The unattached cells were removed, and the plates were filled with PBS, sealed with Parafilm, and centrifuged inverted for 5 min at $300 \times g$ at room temperature using a large capacity tabletop centrifuge (Hanilscience Industrial, Gangneung, Korea). After centrifugation, the detached cells were removed with two PBS washes. The retained cells were fixed with ice-cold 100% methanol for 15 min, washed twice with PBS, stained with crystal violet solution (0.1% crystal violet and 10% ethanol), and gently washed with water until the color stopped rinsing off. The plates were then air-dried; the stained cells were eluted with elution buffer (5% acetic acid and 5% methanol); and absorbance was measured at A_{595} nm using a UV spectrophotometer.

Transwell Migration Assay—The lower surface of Transwell inserts (Costar) was coated with gelatin (10 μg/ml), and the membranes were allowed to dry for 1 h at room temperature. The Transwell inserts were assembled into a 24-well plate, and the lower chamber was filled with α-modified Eagle's medium containing 5% FBS. Cells (8×10^4) were added to each upper chamber, and the plate was incubated at 37 °C in a 5% CO_2 incubator for 16 h. Migrated cells were stained with 0.6% hematoxylin and 0.5% eosin and counted.

Rac Activity Assay—GST-PAK-PBD binding assays were performed essentially as described (21). Briefly, the p21-binding domain of PAK1 (PBD) was expressed in *E. coli* as a GST-PAK-PBD fusion protein and purified using glutathione-agarose beads. The glutathione-agarose bead-bound GST-PBDs were washed with lysis buffer three times and mixed with the transfected HCT116 cell lysates of equal volume and concentration for 2 h at 4 °C. The beads were washed four times with lysis buffer, and bound Rac1 proteins were detected by Western blotting using a polyclonal antibody against Rac1.

Wound-healing Assay—REFs (at consistent cell densities) were transfected with vectors encoding the indicated cDNAs. Approximately 24 h post-transfection, each confluent monolayer was scratched once with a 10-μl pipette tip, washed with PBS to remove detached and damaged cells, and covered with fresh medium. The central region of each scratch was photographed immediately (0 h) and at various time points thereafter, using a ×5 objective lens. During the assay, cells were maintained at 37 °C in a humidified 5% CO_2 atmosphere.

Monitoring Cell Spreading and Migration—Cell spreading and migration were monitored using the xCELLigence system (Roche Applied Science). For cell spreading, E-plate 16 assemblies (Roche Applied Science) were coated with fibronectin (10 μg/ml) and seeded with cells (1.0×10^4 cells/well). Each plate was assembled on the RTCA DP Analyzer (Roche Applied Science), and data were gathered at 5-min intervals for 20 h at 37 °C in 5% CO_2. The obtained data were analyzed using the provided RTCA software. For cell migration, a CIM-Plate 16 (Roche Applied Science) was used. The lower chambers were filled with fresh medium (160 μl/well) with 5% FBS, and the upper chambers were filled with serum-free medium (30 μl/well). The plates were incubated at 37 °C in 5% CO_2 for 1 h, and the background was measured using the RTCA DP analyzer. Transfected cells (1.0×10^4 cells/well) were added to each well, and the plate was incubated at 25 °C for 30 min. The CIM-Plate was then assembled onto the RTCA DP analyzer, and cell migration was assessed at 5-min intervals for 24 h at 37 °C in 5% CO_2. The obtained data were analyzed using the provided RTCA software.

Statistical Analysis—Data are presented as the means from at least three independent experiments. Statistical analysis was performed using an unpaired Student's *t* test. A *p* value less than 0.05, 0.01, or 0.001 was considered statistically significant.

RESULTS

The TMD of Syndecan-2 Has a Stronger Tendency for SDS-resistant Dimerization than That of Syndecan-4—To investigate whether the TMDs of syndecan-2 and -4 have different tendencies for oligomerization, we constructed and expressed several GST-tagged replacement mutants (Fig. 1*A*) and compared their SDS-resistant dimer formation abilities. Consistent with a previous report (13), wild-type syndecan-2 and -4 (SDC2 and SDC4, respectively) formed SDS-resistant dimers, but their TMD mutants (2EPT2C and 4EPT4C, respectively) showed decreased SDS-resistant dimer formation (Fig. 1, *B* and *C*). Mass spectrometry confirmed that the indicated bands correspond to dimers of GST-syndecan-2 proteins (Table 1). Under our experimental conditions, we further noticed that most of the syndecan-2 proteins (94%) formed SDS-resistant dimers, compared with only ~66% of the syndecan-4 proteins (Fig. 1, *B* and *C*). Thus, the dimer/monomer ratio of syndecan-2 was much higher than that of syndecan-4 (see Fig. 3*F*). These results indicate that the syndecan-2 TMD might have a stronger ability to form SDS-resistant dimers compared with that of syndecan-4. Consistent with this notion, a GST-syndecan-2 mutant containing the syndecan-4 TMD (2E4T2C) showed much less SDS-resistant dimer formation than wild-type syndecan-2 (Fig. 1*B*), whereas a GST-syndecan-4 mutant containing the syndecan-2 TMD (4E2T4C) showed enhanced SDS-resistant dimer formation compared with that of wild-type syndecan-4 (Fig. 1*C*). These results indicate that syndecan family members may have different affinities for TMD-TMD association and that the syndecan-2 TMD has a higher tendency to form SDS-resistant dimers compared with the syndecan-4 TMD.

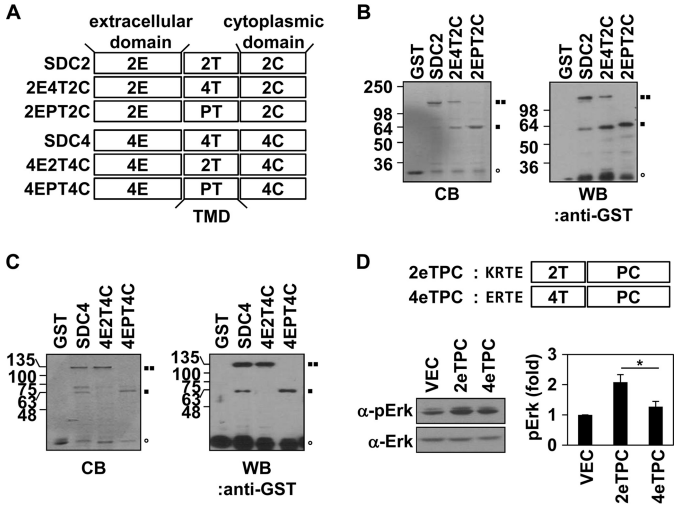

FIGURE 1. **The TMD of syndecan-2 has a stronger tendency to form SDS-resistant dimers compared with the TMD of syndecan-4.** *A*, schematic representation of the syndecan-2 (*top*) and -4 (*bottom*) core proteins. The extracellular (*E*), transmembrane (*T*), and cytoplasmic (*C*) domains are indicated. Syndecan TMD mutants are indicated (2E4T2C, syndecan-2 containing the syndecan-4 TMD; 4E2T4C, syndecan-4 containing the syndecan-2 TMD; and 2EPT2C and 4EPT4C, syndecan-2 and -4, respectively, containing the TMD of human PDGFR). *B* and *C*, recombinant GST-tagged wild-type syndecans (SDC2 and SDC4) or syndecan mutants (2E4T2C, 2EPT2C, 4E2T4C, and 4EPT4C) were purified using glutathione-agarose beads, separated by 10% SDS-PAGE, stained with Coomassie Blue (*CB*, *left*), and detected with an anti-GST antibody (*WB*, *right*). ○, GST cleavage form; ■■, dimer; ■, monomer. *D*, *top*, schematic representations of the 2eTPC and 4eTPC chimeras, in which four amino acid residues of the extracellular domains of rat syndecan-2 (KRTE) or -4 (ERTE) and their corresponding TMDs were linked to the cytoplasmic domain of human PDGFR. *Bottom left*, HEK293T cells expressing 2eTPC, 4eTPC, or empty vector (control) were lysed with radioimmune precipitation assay buffer. Equal amounts of cell lysate were analyzed by Western blot analysis using antibodies against phospho-ERK and ERK. *Bottom right*, quantitative analysis of three independent experiments was performed using the ImageJ program. *, $p < 0.05$ *versus* 2eTPC. *Error bars*, S.D.

Because the syndecan TMD can dimerize by itself in the cell membrane, without requiring the extracellular or cytoplasmic domains (13), we constructed the syndecan chimeras, 2eTPC and 4eTPC, which comprised the TMDs of syndecan-2 or -4, respectively, plus their four flanking extracellular amino acid residues (KRTE and ERTE, respectively) and the cytoplasmic domain of PDGFR (Fig. 1*D*, *top*). Because dimerization of the PDGFR cytoplasmic domain is sufficient to activate MAPK activity (22, 23), MAPK activation was taken as indicating dimerization of these chimeras. Western blotting with an anti-phospho-ERK antibody showed that phosphorylation of ERK was increased in HEK293T cells transfected with both chimeras but that the syndecan-2/4. TMD of syndecan-2 increased the level of phospho-ERK more than the syndecan-4 TMD (Fig. 1*D*, *bottom*). Collectively, these data suggest that the TMDs of syndecan-2 and -4 have different tendencies to form dimers and that the TMD of syndecan-2 has a higher affinity than that of syndecan-4.

The Syndecan-2 TMD Has Unique Regulatory Functions—Because TMD-mediated dimerization is indispensable for the functions of syndecans (13), we hypothesized that the different affinities of their TMDs for intramolecular interaction might affect the cellular functions of syndecan-2 and -4. To investigate this possibility, we first examined the importance of the syndecan-2 TMD for its functions. REFs were transfected with wild-type syndecan-2 or its mutants and plated on fibronectin-coated E-plates, and cell spreading was measured using the xCELLigence system. Our data revealed that overexpression of syndecan-2 in REFs slightly enhanced cell spreading on fibronectin but that this effect was diminished in cells overexpressing syndecan-2 mutants containing the TMDs of syndecan-4 (2E4T2C) or PDGFR (2EPT2C) (Fig. 2*A*). When we monitored cell migration using the xCELLigence system, we found a more evident effect of this TMD replacement. Syndecan-2 overexpression significantly enhanced the migration of REFs compared with the vector control, whereas overexpression of 2E4T2C only slightly enhanced cell migration (Fig. 2*B*). This is interesting given the high sequence homology between the syndecan-2 and -4 TMDs. In addition, another dimerization-defective mutant (2EPT2C) failed to show increased cell migration (Fig. 2*B*). Our wound-healing assays yielded very similar results. At 16 h postwounding, REFs overexpressing syndecan-2 had filled in the scratched area, whereas those transfected with the syndecan-2 mutant containing the syndecan-4 TMD had only partially closed the scratch (Fig. 2*C*). This suggests that proper dimerization of the native TMD of the adhesion receptor, syndecan-2, contributes to regulating cell migration.

Because cell-substratum adhesion plays an important role in cell migration (24, 25), we next investigated whether the syndecan-2 TMD could regulate cell-substratum adhesion, which was quantified using an inverted centrifugal detachment assay. REFs were cultured on a fibronectin-coated plate and detached using inverted centrifugation, and the number of retained cells was analyzed. As expected, the syndecan-2 TMD, but not the TMD of syndecan-4 or PDGFR, enhanced the cell-fibronectin adhesiveness mediated by syndecan-2 overexpression (Fig. 2*D*). Together, these data strongly suggest that each syndecan TMD plays a unique regulatory role, and the syndecan-4 TMD cannot fully mimic the function of the syndecan-2 TMD. Thus, the TMD of syndecan-2 appears to be crucial for the cellular functions of this protein, and at least some of the functional differences between family members may arise from differences in the affinities of their TMDs for intramolecular interaction.

A Unique Phenylalanine Enables the Enhanced Intramolecular Interaction of the Syndecan-2 TMD—To investigate the regulatory mechanism of the syndecan TMDs, we compared their amino acid sequences. The amino acid sequences of TMDs are highly conserved among the members of the syndecan and species including human, mouse, and rat (26). In the case of rat syndecan-4 TMD, it has only two different amino acids compared with human syndecan-4 TMD and five different amino acids compared with rat syndecan-2 TMD. Moreover, syndecan-2 has exactly the same amino acid sequences between each species, including humans, mice, and rats (13, 27). Among the human syndecan paralog TMDs, we found that whereas syndecan-2 has three phenylalanines in its TMD, syndecan-4 has only two. Because it has been reported that phenylalanines in a TMD, especially one harboring the G*XXX*G motif, can enhance TMD-TMD interactions (8), we investigated the roles of these phenylalanines in the dimerization of the syndecan-2 TMD. We generated mutants in which these phenylalanines were substituted with tyrosine (Fig. 3*A*) because tyrosine also contains an aromatic ring and makes π-π interactions in a manner sim-

TABLE 1

GST-tagged recombinant protein was identified to be HSPG core protein (syndecan-2) by mass spectrometry

Shown are LC-MS/MS sequencing results of 44 peptides, all of which are the matched peptides that led to sequence coverage of 42% identification of syndecan-2 core protein (*Rattus norvegicus*). Nominal mass is 23,276 Da, and calculated pI value is 4.64. An underlined M indicates an oxidized methionine residue.

Calculated mass	Expected mass	Δ mass	Start sequence	End sequence	Sequence
Da	*Da*	*Da*			
1384.5344	1383.7038	−0.8306	74	86	GSPDLTTSQLIPR
1384.5344	1384.1463	−0.3881	74	86	GSPDLTTSQLIPR
1384.5344	1384.1741	−0.3604	74	86	GSPDLTTSQLIPR
1384.5344	1384.6521	0.1176	74	86	GSPDLTTSQLIPR
1384.5344	1384.8379	0.3034	74	86	GSPDLTTSQLIPR
1384.5344	1384.9252	0.3907	74	86	GSPDLTTSQLIPR
1384.5344	1384.9620	0.4276	74	86	GSPDLTTSQLIPR
1384.5344	1384.9756	0.4411	74	86	GSPDLTTSQLIPR
1384.5344	1385.0160	0.4815	74	86	GSPDLTTSQLIPR
1384.5344	1385.0356	0.5012	74	86	.GSPDLTTSQLIPR
1384.5344	1385.0627	0.5283	74	86	GSPDLTTSQLIPR
1384.5344	1385.1250	0.5905	74	86	GSPDLTTSQLIPR
1384.5344	1385.2070	0.6726	74	86	GSPDLTTSQLIPR
1384.5344	1385.2178	0.6833	74	86	GSPDLTTSQLIPR
1384.5344	1385.2976	0.7632	74	86	GSPDLTTSQLIPR
1384.5344	1385.5332	0.9988	74	86	GSPDLTTSQLIPR
1690.9528	1690.0410	−0.9118	87	102	ISLTSAAPEVETMTLK
1690.9528	1690.1948	−0.7580	87	102	ISLTSAAPEVETMTLK
1690.9528	1690.6617	−0.2911	87	102	ISLTSAAPEVETMTLK
1690.9528	1690.9221	−0.0307	87	102	ISLTSAAPEVETMTLK
1690.9528	1690.9245	−0.0283	87	102	ISLTSAAPEVETMTLK
1690.9528	1691.2660	0.3131	87	102	ISLTSAAPEVETMTLK
1690.9528	1691.4685	0.5157	87	102	ISLTSAAPEVETMTLK
1690.9528	1691.5537	0.6009	87	102	ISLTSAAPEVETMTLK
1690.9528	1691.5992	0.6464	87	102	ISLTSAAPEVETMTLK
1690.9528	1691.6747	0.7218	87	102	ISLTSAAPEVETMTLK
1690.9528	1691.8188	0.8660	87	102	ISLTSAAPEVETMTLK
1706.9522	1707.2361	0.2838	87	102	ISLTSAAPEVETMTLK
1706.9522	1707.3567	0.4044	87	102	ISLTSAAPEVETMTLK
1706.9522	1707.4454	0.4932	87	102	ISLTSAAPEVETMTLK
2020.1097	2020.7679	0.6581	103	120	TQSITPTQTESPEETDKK
1783.8889	1784.6404	0.7515	137	151	STDVYTEKHSDNLFK
1940.0746	1940.5228	0.4483	137	152	STDVYTEKHSDNLFKR
1140.1145	1140.4730	0.3585	185	194	DEGSYDLGER
2101.1872	2102.0068	0.8196	185	203	DEGSYDLGERKPSSAAYQK
1887.0963	1887.5757	0.4793	195	211	KPSSAAYQKAPTKEFYA
1887.0963	1887.5843	0.4880	195	211	KPSSAAYQKAPTKEFYA
1887.0963	1887.6258	0.5295	195	211	KPSSAAYQKAPTKEFYA
1887.0963	1887.6799	0.5835	195	211	KPSSAAYQKAPTKEFYA
926.0237	926.5670	0.5434	204	211	APTKEFYA
926.0237	926.8963	0.8727	204	211	APTKEFYA

ilar to phenylalanine (28–30). Interestingly, substitution of Phe^{167} to tyrosine in the syndecan-2 TMD (S2(F167Y)) showed reduced dimer formation in SDS-PAGE conditions, although the mutant contained the G*XXX*G motif (Fig. 3*B*). In contrast, neither S2(F169Y) nor S2(F172Y) had this effect (Fig. 3*B*), suggesting that Phe^{167}, the unique phenylalanine, might help to strengthen the syndecan-2 TMD-TMD interaction. Based on this, we speculated that the lower tendency of syndecan-4 for SDS-resistant dimerization might reflect the absence of Phe^{167} in its TMD. To test this, we first replaced Phe^{167} in syndecan-2 with isoleucine, which is found at the corresponding position of the syndecan-4 TMD (S2(F167I)). As expected, S2(F167I) showed decreased SDS-resistant dimer formation compared with wild-type syndecan-2. Notably, however, the SDS-resistant dimer formation of S2(F167I) was higher than that of S2(F167Y) (Fig. 3*C*). In addition, our gel filtration data revealed that syndecan-2 formed higher tetramers than S2(F167I) (Fig. 3*D*), supporting our notion that the presence of Phe^{167} is correlated with a higher tendency toward oligomerization. Consistent with this finding, exchanging Ile^{162} in syndecan-4 with phenylalanine increased the SDS-resistant dimer formation of syndecan-4 (Fig. 3*E*). We next statistically quantified the dimer/total band ratios obtained on SDS-polyacrylamide gels using the ImageJ program. Our results revealed that syndecan-2 showed higher dimer formation ratios than syndecan-4 (SDC2, 94%; SDC4, 66%), and the syndecan-2 substitution mutants, 2E4T2C and S2(F167I), had lower dimer formation ratios than syndecan-2 (2E4T2C, 38%; S2(F167I), 37%). In contrast, the syndecan-4 mutants, 4E2T4C and S4(I162F), had higher dimer formation ratios, comparable with those of syndecan-2 (4E2T4C, 94%; S4(I162F), 97%) (Fig. 3*F*). To further investigate whether the unique phenylalanine residue in syndecan-2 TMD is sufficient for the strong tendency toward syndecan-2 dimer formation, we constructed two additional mutants of syndecan-2, S2(A161V) and S2(I171V). Both of these new mutants showed decreased SDS-resistant dimer formation compared with wild-type syndecan-2, but these reductions were less severe than those seen for the S2(F167I) mutant (Fig. 3*G*). Taken together, these data indicate that Phe^{167} of syndecan-2 strengthens the intramolecular interactions of its TMD.

Phe^{167} Is Critical to the Unique Dimeric Conformation of Syndecan-2—An *in vitro* interaction assay showed that Phe^{167} in the TMD of syndecan-2 is critical to the specific dimerization of syndecan-2. To confirm this finding at the atomic level, we performed NMR spectroscopy. NMR-based chemical shift perturbation experiments are widely used to determine the inter-

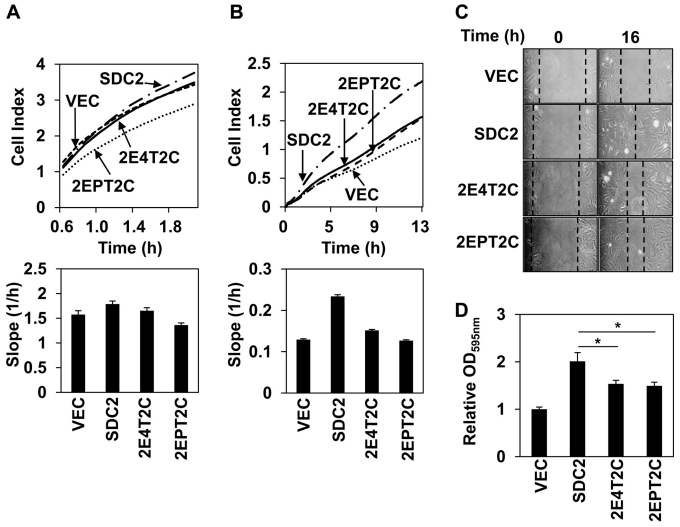

FIGURE 2. **The syndecan-2 TMD is crucial for the function of syndecan-2.** *A*, REFs transfected with empty vector or vectors encoding syndecan-2 or syndecan-2 mutants were plated on E-plates precoated with fibronectin (10 μg/ml). At the indicated times, cell spreading was monitored at intervals of 5 min and plotted using the xCELLigence system. Representative results from three independent experiments are shown. *B*, transfected cells were seeded in duplicate in the upper chambers of CIM-Plates. The lower chambers were filled with medium containing 5% FBS, and migration was monitored and plotted using the xCELLigence system. Representative results from three independent experiments are shown. *C*, transfected REFs were grown to 100% confluence, and these procedures were performed on wound-healing assays as described under "Experimental Procedures." The wound areas were examined and photographed at 0 and 16 h postwounding. *D*, the inverted centrifugal detachment assay (described under "Experimental Procedures") was used to quantify the adhesiveness of transfected REFs to fibronectin. The average absorbance of the empty vector at A_{595} nm is indicated as a control. The data are representative of three independent experiments and are expressed as mean ± S.D. (*error bars*); *, $p < 0.05$ *versus* syndecan-2.

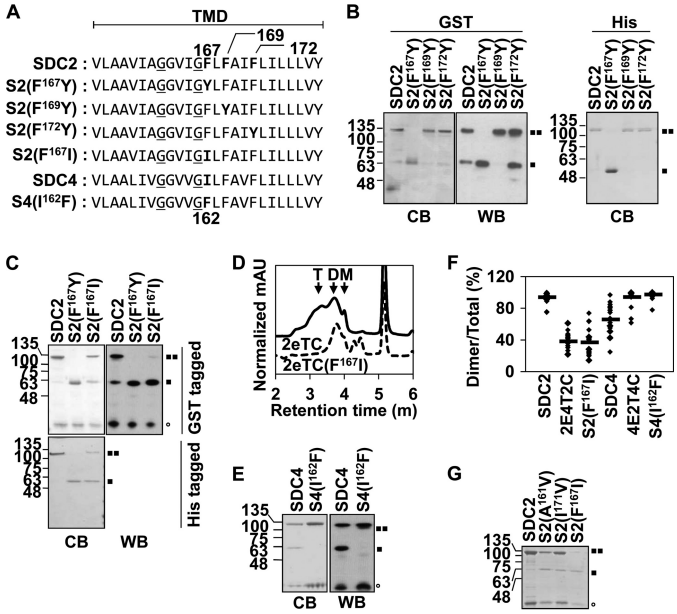

FIGURE 3. **Phe^{167} enhances the SDS-resistant dimer formation of syndecan-2.** *A*, the amino acid sequences of the rat/human syndecan-2 and rat syndecan-4 TMDs are shown. The conserved G*XXX*G motif is *underlined*, and the phenylalanines are shown in *boldface type*. In the syndecan-2 mutants shown, certain phenylalanines were replaced with tyrosine (S2(F167Y), S2(F169Y), and S2(F172Y)) or isoleucine (S2(F167I)); in the syndecan-4 mutant shown, an isoleucine was replaced with a phenylalanine (S4(I162F)). *B*, recombinant GST-tagged (*left* and *middle*) or His-tagged (*right*) wild-type SDC2 or the indicated mutants were purified, separated by SDS-PAGE, and either stained with Coomassie Blue (*CB*) or analyzed by immunoblotting using an anti-GST antibody (*WB*). *C*, *E*, and *G*, the indicated syndecan-2 or syndecan-4 mutants were purified, separated by SDS-PAGE, and either stained with Coomassie Blue or immunoblotted with an anti-GST antibody. Molecular mass markers are shown (in kDa), and the positions of the SDS-resistant syndecan-2 dimers (■■) and monomers (■) and GST (○) are indicated. *D*, the oligomeric states of 2eTC (*black line*) and 2eTC(F167I) (*dotted black line*) were measured by analytical size exclusion gel chromatography traces. The elution positions of monomeric (*M*), dimeric (*D*), and tetrameric (*T*) 2eTC are indicated. All peaks were detected by a 280-nm wavelength, and peak intensities were normalized by protein concentration. *F*, quantitative analysis of 20 stained dimer/monomer syndecan bands was performed using the ImageJ program. The average levels are indicated by *horizontal bars*.

action sites between two molecules and/or the conformational changes associated with their interaction. Here, unlabeled 2eTC and 2eTC(F167I) mutant proteins were titrated with labeled syndecan-2 TMDs at different molar ratios. The ^{1}H-^{15}N cross-peaks in the two-dimensional HSQC spectrum of the syndecan-2 TMD did not show any significant shift in the 2eTC titration, indicating that there was no dramatic conformational change (Fig. 4). In contrast, titration of the syndecan-2 TMD with 2eTC(F167I) yielded dramatic shifts in several cross-peaks, indicating that the conformation of the syndecan-2 TMD was perturbed by the interaction (Fig. 4). Under close inspection, Phe^{167} and Phe^{172} showed dramatic chemical shifts in the syndecan-2 TMD/2eTC(F167I) titration, whereas Phe^{169}, which is conserved in the syndecan family, showed only a small shift. Taken together, these findings suggest that the unique dimeric conformation of syndecan-2 might be altered by the F167I mutation; especially, larger conformational changes are induced in Phe^{167} or Phe^{172} *versus* Phe^{169} (Fig. 4*A*). In a similar manner, perturbation of the chemical shift in several residues located in the C terminus of the transmembrane was observed. As in Fig. 4*A*, a stepwise chemical shift was detected by titrating increased concentrations of 2eTC(F167I), whereas no change was observed in 2TM when wild-type 2eTC was titrated (Fig. 4*B*). These results demonstrate that Phe^{167} might not only drive the unique conformation of the syndecan-2 TMD dimer; it may also affect the dimerization of the cytosolic region, thereby potentially regulating the interaction of syndecan-2 with some of its target molecules within the cell. Together, the results from our NMR titration experiments demonstrate that syndecan-2 maintains its unique conformation in complex with 2eTC but shows major conformational changes when complexed with the 2eTC (F167I) mutant (Fig. 4*C*).

Phe^{167} of Syndecan-2 Affects Its Cellular Functions—Finally, we investigated whether Phe^{167} of syndecan-2 was involved in regulating the functions of syndecan-2. Because the transfected syndecan-2 constructs were expressed at similar levels and formed homodimers on the cell surface (Fig. 5, *A* and *B*), these cDNA constructs were introduced into REF cells. Transwell migration assays showed that, whereas REFs transfected with wild-type syndecan-2 increased cell migration compared with vector control cells, the migration levels of REFs transfected with either 2E4T2C or S2(F167I) were greatly reduced (Fig. 5*C*). Wound-healing assays yielded similar results (Fig. 5*D*), and the interaction of syndecan-2 with fibronectin was decreased in cells overexpressing 2E4T2C or S2(F167I) compared with those overexpressing wild-type syndecan-2 (Fig. 5*F*) without changing the expression of integrins (Fig. 5*E*). To exclude the effects

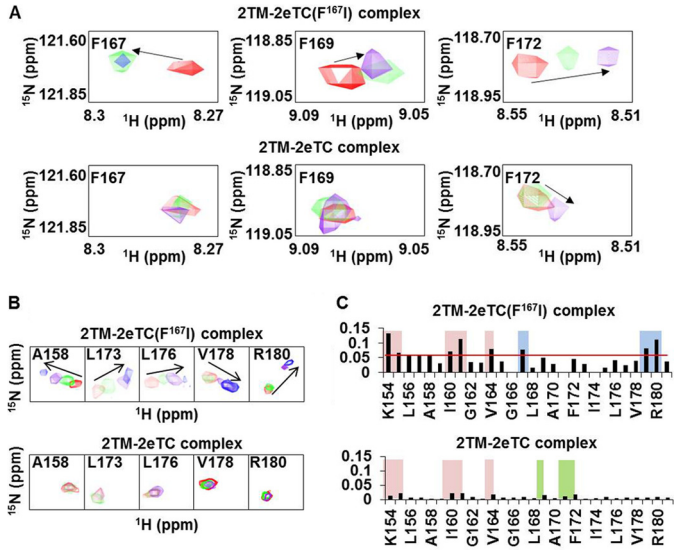

FIGURE 4. **The F167I mutant of syndecan-2 shows a different binding mode during dimerization.** *A*, NMR titrations were performed with ^{15}N-labeled 2TM and 2eTC or 2eTC(F167I) at up to a 1:3 molar ratio. Data from titration experiments are shown in *red* (1:0), *green* (1:1), *purple* (1:2), and *blue* (1:3). The chemical shift perturbations of Phe^{167} (*left*), Phe^{169} (*center*), and Phe^{172} (*right*) were assessed by overlapping the three titration points and are shown for the 2TM-2eTC(F167I) complex (*top*) and the 2TM-2eTC complex (*bottom*). *B*, chemical shift comparison among 2TM-2eTC(F167I), and 2TM-2eTC. *C*, NMR chemical shift perturbation of 2TM during titrations with 2eTC(F167I) (*top*) or 2eTC (*bottom*) at a molar ratio of 1:3, as calculated using the equation, $\Delta\delta_{AV} = ((\Delta\delta_{1H})^2 + (\Delta\delta_{15N}/5)^2)^{1/2}$, where $\Delta\delta_{AV}$, $\Delta\delta_{1H}$, and $\Delta\delta_{15N}$ represent average chemical shift value, proton chemical shifts, and nitrogen chemical shift changes, respectively.

of endogenous syndecans, HCT116 cells were subjected to siRNA-mediated knockdown of syndecan-2 (human SDC2) and then transfected with an expression vector encoding the rat syndecan-2 cDNA. Migration assays were performed on HCT116 cells re-expressing either wild-type or mutant syndecan-2 proteins. Both mutants triggered much less cell migration activity compared with that initiated by wild-type syndecan-2 (Fig. 5*G*).

Because MAPK activation could be used as an indicator of dimerization (Fig. 1*D*), we also compared the levels of phospho-ERK in cells overexpressing wild-type or mutant versions of syndecan-2 (Fig. 5*H*). As expected, cells overexpressing 2eT(F167I)PC showed reduced phosphorylation of ERK compared with those overexpressing 2eTPC (Fig. 5*H*). Syndecan-2 expression has been shown to regulate the migration of colon cancer cells through Tiam1-dependent Rac1 activation (17), and syndecan-2 dimerization was found to play a fundamental role in this signaling (17, 18). Consistent with this, we found that wild-type syndecan-2 promoted the activation (GTP binding) of Rac1 in HCT116 cells, whereas S2(F167I) and 2E4T2C had much more limited effects (Fig. 5*I*). Because our results suggested that the absence of Phe at the 162nd amino acid position of syndecan-4 (the position corresponding to Phe^{167} in the syndecan-2 TMD) may form the basis for the functional differences between the TMDs of syndecan-2 and -4, we replaced the isoleucine in 2E4T2C with phenylalanine and examined the dimerization and functions of the resulting protein. Overexpression of the generated mutant, 2E4T2C(I162F), significantly rescued the SDS-resistant dimer formation (to 96%; Fig. 6, *A* and *B*), adhesive force to fibronectin (Fig. 6*C*), cell migration ability (Fig. 6, *D* and *E*), and Rac1 activation activity (Fig. 6*F*) with respect to 2E4T2C. Moreover, compared with 4eTPC, 4eT(I162F) showed enhanced phosphorylation of ERK (Fig. 6*G*). Collectively, these results suggest that Phe^{167} is a key amino acid residue that gives syndecan-2 some of its unique functions.

DISCUSSION

Intramembrane protein-protein interactions of cell surface receptors are involved in many vital cellular processes. However, in contrast to the soluble cytoplasmic and extracellular domains, the TMD has received far less attention. Although the TMD is known to be involved in regulating receptor dimerization/oligomerization, we know little about the factors that control the dimerization/oligomerization of TMDs. Syndecans are known to self-associate through their conserved TMDs (13, 14). Furthermore, a conserved G*XXX*G motif in the TMD is thought to enable the formation of stable TMD dimers, which is crucial for the functions of syndecan-2 and -4 (13). A previous study using synthetic peptides corresponding to the TMDs of the various syndecan family members showed that they differed in their tendencies to form SDS-resistant TMD dimers (14). Together, these previous studies suggested that the syndecan TMD may play a specific role in the functional regulation of syndecans.

Indeed, our present results revealed that the TMD is important for various functions of syndecan-2, including the mediation of migration and cell-substratum adhesiveness (Fig. 2). In contrast, the syndecan-4 TMD, which is highly homologous to that of syndecan-2, was unable to mimic the functions of the syndecan-2 TMD (Figs. 1 and 2). These data indicate that although the syndecan TMDs are highly homologous, they each may have unique regulatory functions conveyed via distinct mechanisms.

We hypothesized that the TMDs could regulate the functions of syndecan family members through their affinities for intramolecular interactions. Indeed, chimeric proteins in which the TMD of syndecan-2 was replaced with those of syndecan-4 or PDGFR showed greatly reduced SDS-resistant dimer formation, and our biochemical results indicated that the TMD of syndecan-2 had a higher dimerization affinity compared with the other tested TMDs (Fig. 1). Our results confirmed that the syndecan TMD can self-associate through the G*XXX*G motif independent of the extracellular and cytoplasmic domains and additionally showed that the syndecan TMDs differ in their dimerization affinities. This led us to speculate that certain non-conserved amino acids might regulate the self-associations of the syndecan-2 and -4 TMDs.

The regulation of TMD-mediated GpA (glycophorin A) dimerization involves the G*XXX*G motif and appears to be further stabilized by the interaction of amino acids near the G*XXX*G motif and/or interfacial amino acids of the helix (4, 6–8). In particular, aromatic residues (*e.g.* phenylalanine, tyrosine, and tryptophan) are involved in π-π and cation-π interactions (28–30), and the formation of such interactions between planar aromatic rings seems to be essential for the assembly of soluble proteins (31, 32). Moreover, the presence of

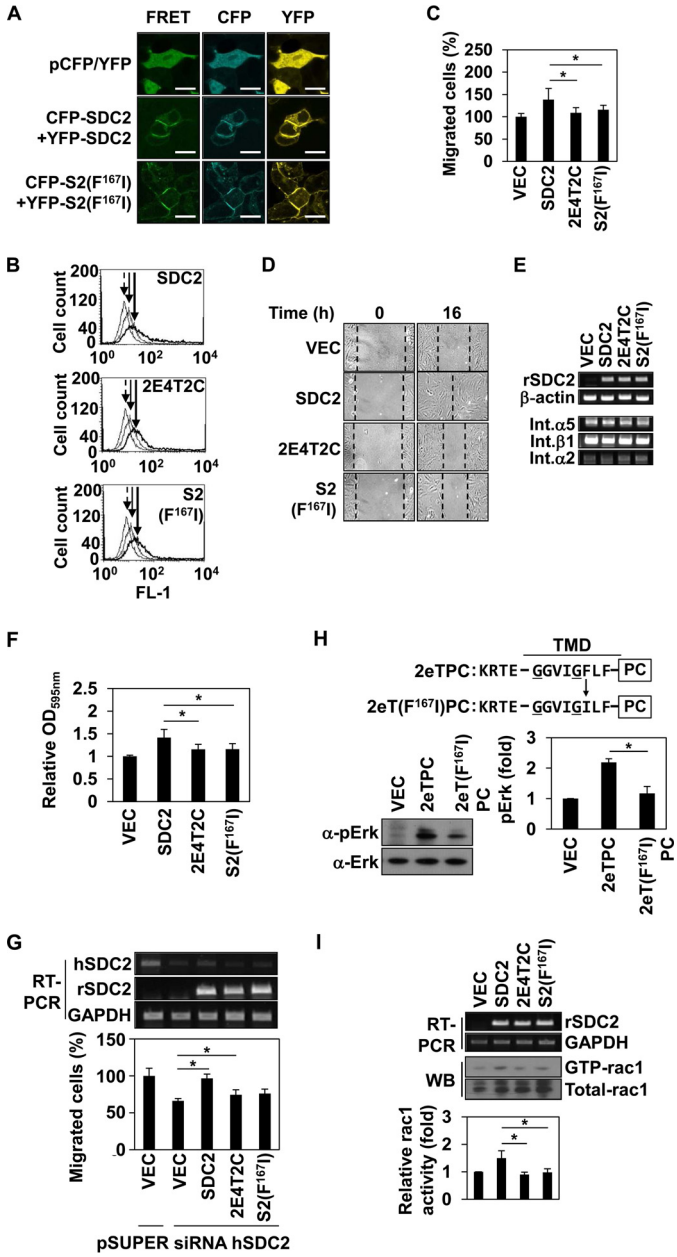

FIGURE 5. **Phe^{167} is critical to syndecan-2-mediated cell functions.** *A*, HEK293T cells were transiently co-transfected with indicated cDNAs expressing SDC-CFP and SDC-YFP constructs. After 48 h post-transfection, the cells were fixed using 3.5% paraformaldehyde, and images were captured by confocal microscopy using a filter set specific for CFP, YFP, and FRET. *Bar*, 10 μm. *B*, transfected REF cells were analyzed by flow cytometry as described under "Experimental Procedures." *Arrow* with *dotted line*, IgG; *arrow* with *solid line*, vector; *arrow* with *thick line*, syndecan-2 or mutant constructs. *C*, REFs were transfected with empty vector or those encoding syndecan-2 or the indicated syndecan-2 mutants in serum-free medium and seeded to the upper chamber of a transwell apparatus. The lower chamber was filled with serum-containing medium. At 16 h postseeding, migrated cells were stained with hematoxylin and eosin. The data shown are representative of three independent experiments; *, $p < 0.05$ *versus* syndecan-2. *D*, wound-healing assays were performed with transfected REFs. The wound areas were examined and photographed at 0 and 16 h post-wounding. *E*, REF cells were transfected with syndecan-2, vector, and mutant constructs. After 24 h, RT-PCR for transfection efficiency and expression of integrins was performed. *F*, inverted centrifugal detachment assays were performed on REFs expressing syndecan-2 or the indicated syndecan-2 mutants. The data shown are representative of four independent experiments; *, $p < 0.05$ *versus* syndecan-2. *G*, HCT-116 cells were down-regulated by using pSuper vector targeting human syndecan-2 (*siRNA hSDC2*) or empty pSuper vector, simultaneously, and were co-overexpressed with rat syndecan-2 or syndecan-2 mutant constructs. We performed RT-PCR for transfection efficiency and transwell migration. The data shown are representative of three independent experiments; *, $p < 0.05$. *H*, *top*, schematic representations of the 2eTPC and 2eT(F167I)PC chimeras used in these experiments. Four flanking amino acids of the extracellular domain of rat syndecan-2 (KRTE) and the TMD of a syndecan-2 single point mutant (S2(F167I)) were linked to the cytoplasmic domain of human PDGFR. *e*, the flanking amino acids of the extracellular domain; *T*, transmembrane domain; *PC*, PDGFR cytoplasmic domain. *Bottom left*, HEK293T cells overexpressing the indicated constructs were analyzed as described in the legend to Fig. 1*D*. *Bottom right*, quantitative analysis of three independent experiments was performed using the ImageJ program. *, $p < 0.05$ *versus* 2eTPC. *I*, Rac activity assay were performed with transfected HCT116 cells. Total cell lysates were used as a positive control (*middle*), the transfection efficiency was analyzed by RT-PCR (*top*), and quantitative analysis of three independent experiments was performed. *, $p < 0.05$ *versus* SDC2. *Error bars*, S.D.

a phenylalanine in addition to the *GXXXG* motif enhances the self-association of the GpA TMD (8). Several other reports have confirmed that aromatic residues, either alone or near the *GXXXG* motif, can stabilize the TMD helix dimerization of membrane proteins (8, 29, 30). Unterreitmeier *et al.* (8) analyzed self-assembling TMDs using a large library of randomized amino acid sequences and found a relationship between enrichment of phenylalanine and high self-association of TMDs.

Interestingly, there are different numbers of phenylalanines in the TMDs of the syndecan family members. For instance, syndecan-2 has three phenylalanines in its TMD (Phe^{167}, Phe^{169}, and Phe^{172}), but syndecan-4 has only two (Phe^{164} and Phe^{167}). Therefore, we speculated that, as in the other studied receptors, phenylalanine might be involved in regulating the interaction strength of the syndecan TMDs. Indeed, syndecan-2, which among the syndecans showed the strongest tendency to form SDS-resistant dimers (14), has a unique Phe^{167} that allows the syndecan-2 TMD to make additional intramolecular interactions (Fig. 3). Loss of Phe^{167} diminished the tendency of syndecan-2 to form SDS-resistant dimers (*i.e.* to less than that of syndecan-4), whereas replacement of the corresponding isoleucine in syndecan-4 with phenylalanine enhanced the SDS-resistant dimer formation of syndecan-4 (Fig. 3). These findings indicate that this phenylalanine residue stabilizes the *GXXXG* motif-mediated dimerization/oligomerization of the syndecan-2 TMD. Notably, the two other phenylalanines in the TMD of syndecan-2 did not appear to be involved in this effect. This might reflect differences in the abilities of these residues to undergo intrahelix associations with other aromatic residues.

Substitution of Phe^{167} with isoleucine reduced SDS-resistant dimer formation and syndecan-2-mediated cell functions, including cell migration. Conversely, Phe substitution of Ile^{162} in syndecan-2 mutant containing syndecan-4 TMD (2E4T2C(I162F)) enhanced its adhesion signaling functions. These findings show that the syndecan TMD contributes to mediating the biological functions of syndecans via (at least in part) a critical phenylalanine.

Interestingly, the presence of Phe^{167} in syndecan-2 was associated with unique structural characteristics in the C-terminal region (Fig. 4). The unique dimeric conformation of syndecan-2 was altered in F167I mutant syndecan-2, as shown by chemical shifts of several residues located in the C-terminal region of the TMD (Fig. 4, *A* and *B*). Because C-terminal amino acid residues are directly connected to the cytoplasmic domain, it is conceiv-

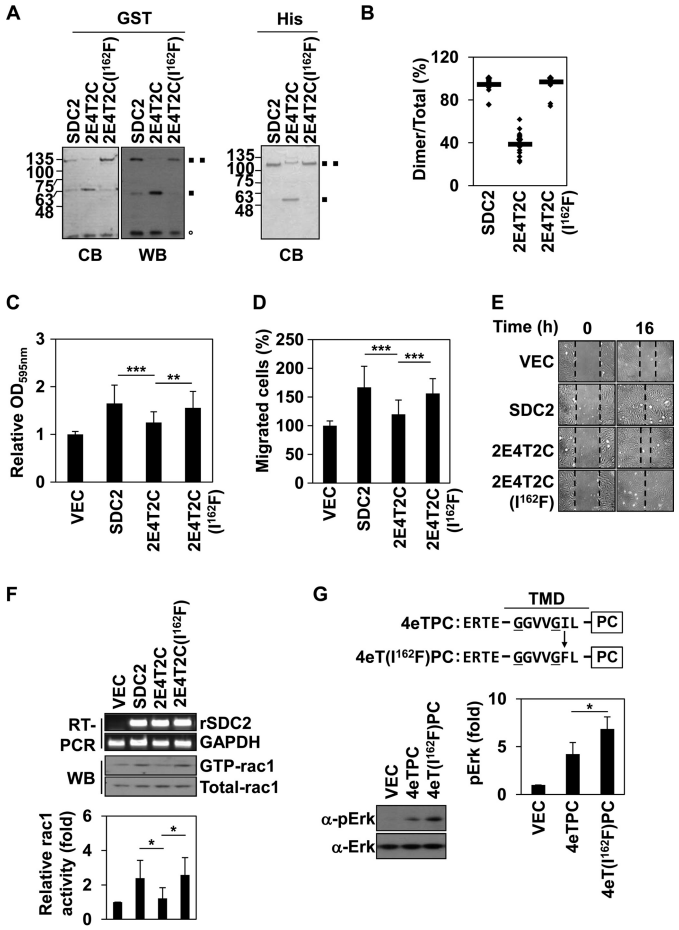

FIGURE 6. **Phe^{167} enhances the TMD dimerization and dimerization-mediated functions of syndecan-4.** *A*, recombinant GST-tagged (*left* and *middle*) or His-tagged (*right*) wild-type SDC2 or the indicated syndecan-2 mutants were purified, separated by SDS-PAGE, and either stained with Coomassie Blue or analyzed by immunoblotting using an anti-GST antibody. Molecular mass markers (in kDa) are shown, and the positions of the SDS-resistant syndecan-2 dimers (■■) and monomers (■) and GST (○) are indicated. *B*, quantitative analysis of 20 stained dimer/monomer syndecan bands was performed using the ImageJ program. The average levels are indicated by *horizontal bars*. *C*, inverted centrifugal detachment assays were performed on REFs expressing wild-type syndecan-2 or the indicated syndecan-2 mutants. The data shown are representative of seven independent experiments. ***, $p < 0.001$; **, $p < 0.01$ *versus* 2E4T2C. *D*, procedures on REFs that were transfected with empty vector or those encoding syndecan-2 or the indicated syndecan-2 mutants were performed using transwell migration. The data shown are representative of six independent experiments. ***, $p < 0.001$ *versus* 2E4T2C. *E*, wound-healing assays were performed on REFs expressing wild-type syndecan-2 or the indicated syndecan-2 mutants. The wound areas were examined and photographed at 0 and 16 h postwounding. *F*, procedures on HCT116 cells transfected with empty vector or those encoding syndecan-2 or the indicated syndecan-2 mutants were performed on Rac activity assays. Total cell lysates were used as a positive control (*middle*), the transfection efficiency was analyzed by RT-PCR (*top*), and quantitative analysis of three independent experiments was performed. *, $p < 0.05$ *versus* 2E4T2C. *G*, *top*, schematic representation of the 4eTPC and 4eT(I162F)PC chimeras. Four flanking amino acids of the extracellular domain of rat syndecan-4 (ERTE) and the TMD of syndecan-4 harboring a single point mutation (S4(I162F)) were linked to the cytoplasmic domain of human PDGFR. *Bottom left*, HEK293T cells overexpressing the indicated constructs were analyzed as described in the legend to Fig. 1*D*. *Bottom right*, quantitative analysis of three independent experiments was performed using the ImageJ program. *, $p < 0.05$ *versus* 4eTPC. *Error bars*, S.D.

able that an additional phenylalanine in the TMD of syndecan-2 could cause alteration of oligomeric status of the cytoplasmic domains of syndecans. Indeed, we observed that syndecan-2-mediated Rac activity and cell migration were reduced following substitution of Phe^{167} (Fig. 5). We previously showed that the oligomeric status of the TMD affects that of the syndecan-4 cytoplasmic domain (15, 16). Therefore, the existence of an additional phenylalanine and the stronger intramolecular interaction of its TMD may affect the oligomeric status of the syndecan-2 cytoplasmic domain, altering its functions as a cell surface receptor.

Collectively, our present results show for the first time that a unique phenylalanine (Phe^{167}) in syndecan-2 increases the *GXXXG*-mediated affinity of its TMD for intramolecular interaction, enhancing the TMD oligomerization that is crucial for the functions of syndecan-2. Future work is warranted to examine how differences in TMD affinity directly regulate the unique functions of each syndecan family member. We speculate that this may occur through changes in the oligomeric status of the cytoplasmic and/or extracellular domains, which would alter their interactions with signaling molecules. Additional work is also needed to study the involvement of TMD-mediated signaling in syndecan-related diseases, such as cancers.

REFERENCES

1. Heldin, C. H. (1995) Dimerization of cell surface receptors in signal transduction. *Cell* **80,** 213–223
2. Schlessinger, J. (2000) Cell signaling by receptor tyrosine kinases. *Cell* **103,** 211–225
3. Fink, A., Sal-Man, N., Gerber, D., and Shai, Y. (2012) Transmembrane domains interactions within the membrane milieu: principles, advances and challenges. *Biochim. Biophys. Acta* **1818,** 974–983
4. Lemmon, M. A., Flanagan, J. M., Hunt, J. F., Adair, B. D., Bormann, B. J., Dempsey, C. E., and Engelman, D. M. (1992) Glycophorin A dimerization is driven by specific interactions between transmembrane α-helices. *J. Biol. Chem.* **267,** 7683–7689
5. MacKenzie, K. R., Prestegard, J. H., and Engelman, D. M. (1997) A transmembrane helix dimer: structure and implications. *Science* **276,** 131–133
6. Dawson, J. P., Melnyk, R. A., Deber, C. M., and Engelman, D. M. (2003) Sequence Context strongly modulates association of polar residues in transmembrane helices. *J. Mol. Biol.* **331,** 255–262
7. Melnyk, R. A., Kim, S., Curran, A. R., Engelman, D. M., Bowie, J. U., and Deber, C. M. (2004) The affinity of *GXXXG* motifs in transmembrane helix-helix interactions is modulated by long-range communication. *J. Biol. Chem.* **279,** 16591–16597
8. Unterreitmeier, S., Fuchs, A., Schäffler, T., Heym, R. G., Frishman, D., and Langosch, D. (2007) Phenylalanine promotes interaction of transmembrane domains via GxxxG motifs. *J. Mol. Biol.* **374,** 705–718
9. Tkachenko, E., Rhodes, J. M., and Simons, M. (2005) Syndecans: new kids on the signaling block. *Circ. Res.* **96,** 488–500
10. Choi, Y., Chung, H., Jung, H., Couchman, J. R., and Oh, E. S. (2011) Syndecans as cell surface receptors: unique structure equates with functional diversity. *Matrix Biol.* **30,** 93–99
11. Rapraeger, A. C. (2000) Syndecan-regulated receptor signaling. *J. Cell Biol.* **149,** 995–998
12. Lambaerts, K., Wilcox-Adelman, S. A., and Zimmermann, P. (2009) The signaling mechanisms of syndecan heparan sulfate proteoglycans. *Curr. Opin. Cell Biol.* **21,** 662–669
13. Choi, S., Lee, E., Kwon, S., Park, H., Yi, J. Y., Kim, S., Han, I. O., Yun, Y., and Oh, E. S. (2005) Transmembrane domain-induced oligomerization is crucial for the functions of syndecan-2 and syndecan-4. *J. Biol. Chem.* **280,** 42573–42579
14. Dews, I. C., and Mackenzie, K. R. (2007) Transmembrane domains of the syndecan family of growth factor coreceptors display a hierarchy of homotypic and heterotypic interactions. *Proc. Natl. Acad. Sci. U.S.A.* **104,** 20782–20787
15. Choi, Y., Kim, S., Lee, J., Ko, S. G., Lee, W., Han, I. O., Woods, A., and Oh, E. S. (2008) The oligomeric status of syndecan-4 regulates syndecan-4

interaction with α-actinin. *Eur. J. Cell Biol.* **87,** 807–815
16. Choi, Y., Kang, D., Han, I. O., and Oh, E. S. (2012) Hierarchy between the transmembrane and cytoplasmic domains in the regulation of syndecan-4 functions. *Cell. Signal.* **24,** 1522–1530
17. Choi, Y., Kim, H., Chung, H., Hwang, J. S., Shin, J. A., Han, I. O., and Oh, E. S. (2010) Syndecan-2 regulates cell migration in colon cancer cells through Tiam1-mediated Rac activation. *Biochem. Biophys. Res. Commun.* **391,** 921–925
18. Lee, H., Kim, Y., Choi, Y., Choi, S., Hong, E., and Oh, E. S. (2011) Syndecan-2 cytoplasmic domain regulates colon cancer cell migration via interaction with syntenin-1. *Biochem. Biophys. Res. Commun.* **409,** 148–153
19. Ryu, H. Y., Lee, J., Yang, S., Park, H., Choi, S., Jung, K. C., Lee, S. T., Seong, J. K., Han, I. O., and Oh, E. S. (2009) Syndecan-2 functions as a docking receptor for pro-matrix metalloproteinase-7 in human colon cancer cells. *J. Biol. Chem.* **284,** 35692–35701
20. Hienola, A., Tumova, S., Kulesskiy, E., and Rauvala, H. (2006) *N*-Syndecan deficiency impairs neural migration in brain. *J. Cell Biol.* **174,** 569–580
21. Hecker, T. P., Grammer, J. R., Gillespie, G. Y., Stewart, J. Jr., and Gladson, C. L. (2002) Focal adhesion kinase enhances signaling through the Shc/extracellular signal-regulated kinase pathway in anaplastic astrocytoma tumor biopsy samples. *Cancer Res.* **62,** 2699–2707
22. Schlesinger, T. K., Demali, K. A., Johnson, G. L., and Kazlauskas, A. (1999) Platelet-derived growth factor-dependent association of the GTPase-activating protein of Ras and Src. *Biochem. J.* **344,** 519–526
23. DeMali, K. A., Balciunaite, E., and Kazlauskas, A. (1999) Integrins enhance platelet-derived growth factor (PDGF)-dependent responses by altering the signal relay enzymes that are recruited to the PDGF β receptor. *J. Biol. Chem.* **274,** 19551–19558
24. Calof, A. L., and Lander, A. D. (1991) Relationship between neuronal migration and cell-substratum adhesion: laminin and merosin promote olfactory neuronal migration but are anti-adhesive. *J. Cell Biol.* **115,** 779–794
25. Montell, D. J. (2008) Morphogenetic cell movements: diversity from modular mechanical properties. *Science* **322,** 1502–1505
26. Carey, D. J. (1997) Syndecans: multifunctional cell-surface co-receptors. *Biochem. J.* **327,** 1–16
27. Chen, L., Couchman, J. R., Smith, J., and Woods, A. (2002) Molecular characterization of chicken syndecan-2 proteoglycan. *Biochem. J.* **366,** 481–490
28. Waters, M. L. (2002) Aromatic interactions in model systems. *Curr. Opin. Chem. Biol.* **6,** 736–741
29. Sal-Man, N., Gerber, D., Bloch, I., and Shai, Y. (2007) Specificity in transmembrane helix-helix interactions mediated by aromatic residues. *J. Biol. Chem.* **282,** 19753–19761
30. Johnson, R. M., Hecht, K., and Deber, C. M. (2007) Aromatic and cation-π interactions enhance helix-helix association in a membrane environment. *Biochemistry* **46,** 9208–9214
31. Kannan, N., and Vishveshwara, S. (2000) Aromatic clusters: a determinant of thermal stability of thermophilic proteins. *Protein Eng.* **13,** 753–761
32. Gazit, E. (2002) A possible role for pi-stacking in the self-assembly of amyloid fibrils. *FASEB J.* **16,** 77–83